

Expression profile of cerebellar proteins in Balb/c mice maintained on a high-carbohydrate diet and treated with glibenclamide

Abstract

The consumption of diets rich in refined carbohydrates is closely associated with rising obesity rates and metabolic disruptions, such as type 2 *diabetes mellitus*, which is commonly managed with glibenclamide. Emerging evidence suggests that the cerebellum may participate in metabolic regulation and respond to both dietary and pharmacological interventions. This study evaluated protein expression profiles in the cerebellum of 16 male Balb/c mice (n = 4 per group) subjected to a standard diet, refined carbohydrate-rich diet, glibenclamide treatment (20 mg/kg), or in combination, and the respective controls for eight weeks. Cerebellar supernatant samples were analyzed using biochemical techniques (SDS-PAGE) and *in silico* predictive assays. Eight distinct protein bands were identified (P1–P8). Glibenclamide administration down-regulated the expression of bands P1 and P3, whereas the high-carbohydrate diet up-regulated them ($p < 0.05$). Band P6 expression decreased significantly under both individual treatments ($p < 0.05$). Conversely, P7 expression decreased exclusively following glibenclamide treatment, while P8 expression was enhanced solely by the dietary intervention ($p < 0.05$). Functional annotation indicated that 28.2% of these predicted proteins are involved in DNA and RNA processing events. In conclusion, a high-carbohydrate diet and glibenclamide independently modulate the cerebellar proteome without exhibiting a significant associated or synergistic interaction.

Keywords: isocaloric diet, electrophoretic profile, Nervous system

Volume 9 Issue 1 - 2026

Isadora de Lima e Silva,¹ Alexandre Azenha Alves de Rezende,¹ Stéfany Bruno de Assis Cau,² Luciana Karen Calábria¹

¹Institute of Exact and Natural Sciences of Pontal, Federal University of Uberlândia, Ituiutaba, MG, Brazil

²Department of Pharmacology, Institute of Biological Sciences, Federal University of Minas Gerais, MG, Brazil

Correspondence: Luciana Karen Calábria, Institute of Exact and Natural Sciences of Pontal, Federal University of Uberlândia, Rua 20, 1600, Tupã, Ituiutaba, MG, Brazil, Tel 55-34 32715252

Received: May 28, 2026 | **Published:** June 16, 2026

Introduction

According to the World Health Organization (WHO), obesity is defined as a chronic, progressive disease characterized by an excessive accumulation of body adipose tissue, driven by a complex interplay of genetic factors and dietary habits. This pathological condition markedly elevates the relative risk of developing severe comorbidities, including type 2 *diabetes mellitus*, arterial hypertension, and various neoplastic processes. Global surveillance data indicate that obesity currently affects over 1 billion individuals worldwide. Projections by the WHO suggest that approximately 167 million people—spanning pediatric, adolescent, and adult populations—will experience severely compromised health outcomes as a direct consequence of being overweight or obese.¹ In the Brazilian context, adult obesity rates have climbed dramatically, rising from 11.8% in 2006 to 25.7% in 2024.²

In this metabolic landscape, the chronic consumption of diets rich in refined carbohydrates serves as a major driver of obesity. Extensive clinical and epidemiological evidence demonstrates that high-carbohydrate eating patterns substantially increase the susceptibility to obesity, cardiovascular diseases, and type 2 *diabetes mellitus*.³ Mechanistically, these diets trigger sustained hyperinsulinemia, which selectively favors peripheral fat storage and inhibits lipolysis.⁴ Furthermore, high-carbohydrate intake has been shown to impair mitochondrial respiration in adipose tissue, which suppresses lipid oxidation rates and exacerbates adiposity.⁵

To counteract the metabolic dysregulation associated with obesity and type 2 *diabetes mellitus*, the sulfonylurea derivative glibenclamide is widely prescribed. Glibenclamide stimulates pancreatic beta-cells to secrete insulin, thereby facilitating systemic glycemic control.⁶ Beyond its primary peripheral hypoglycemic function, glibenclamide exhibits prominent neuroprotective properties. These include the

prevention of cerebral edema,⁷ mitigation of cognitive decline associated with natural aging,⁸ and protection against carbohydrate-induced cardiac remodeling.⁹ Glibenclamide is also an invaluable tool for dissecting neuroprotective and metabolic signaling pathways, such as those activated during a ketogenic diet, which depend on signaling through ATP-sensitive potassium channels (K_{ATP}) in the central nervous system.¹⁰

These neuroprotective effects are highly relevant in the cerebellum, a structure characterized by a remarkably high density of sulfonylurea receptors and functional K_{ATP} channel subunits.¹¹ Within this region, glibenclamide modulates proteins critical for cellular signaling and glucose metabolism, such as phosphoglycerate kinase and the Gs protein alpha-subunit, pointing to a regulatory role in maintaining energy balance and preserving highly specialized populations, such as Purkinje neurons.¹² Ontogenetically, cerebellar sulfonylurea receptor expression is tightly regulated during development; neonatal mice display minimal expression, which rapidly matures to adult levels within the first two weeks of life,¹³ implying a synchronized functional maturation of this pathway.

Although traditionally recognized primarily for its role in motor coordination and balance, the cerebellum contains more than half of the total neuronal population in the central nervous system and is increasingly recognized for its contribution to higher-order cognitive and systemic metabolic functions.¹⁴ This architecture makes the cerebellum highly sensitive to nutritional fluctuations during critical developmental windows. For instance, maintaining pregnant dams on an isocaloric, low-protein diet (8%) triggers a significant reduction in offspring cerebellar weight alongside permanent alterations in total DNA, protein, and lipid concentrations.¹⁵ The cerebellum is also vulnerable to oxidative stress induced by obesogenic diets rich in saturated fats, which can lead to the carbonylation of essential proteins driving ATP homeostasis and glutamate metabolism.¹⁶

The cerebellar response to distinct dietary models displays strict regional and molecular specificity. For example, a ketogenic diet induces localized glucose hypermetabolism in specific cerebellar lobes, contrasting sharply with the reduced glucose uptake observed across other brain regions,¹⁷ while simultaneously stimulating global protein phosphorylation cascades in the cerebellum, cerebral cortex, and hippocampus.¹⁸ Conversely, high-saturated-fat diets promote oxidative stress and protein carbonylation,¹⁶ though certain neurochemical cascades in the cerebellum exhibit striking resilience. The cerebellar cholinergic system, for instance, maintains stable acetylcholinesterase activity even under conditions that disrupt cortical and hippocampal pathways.¹⁹

While it is established that the cerebellum remodels its protein expression profile in response to motor learning and physical stimuli,²⁰ our understanding of how metabolic challenges and pharmacological interventions alter the cerebellar proteome remains restricted. Prior studies have established the systemic metabolic impacts of carbohydrate-rich diets^{9,21} and their broader effects on whole-brain proteomes.^{12,22,25} However, literature specific to cerebellar protein remodeling under nutritional stress is scarce. To address this gap, the present study used biochemical and *in silico* analyses of cerebellar homogenates from Balb/c mice maintained on a refined carbohydrate-rich diet for eight weeks to elucidate differential protein expression and map the modulatory effects of glibenclamide within this specialized tissue.

Methodology

Animal experimentation and ethical approval: Animal procedures were carried out using six-week-old male Balb/c mice at the Animal Facility Center of the Institute of Biological Sciences, Federal University of Minas Gerais (UFMG) in 2017. Animals were housed under tightly controlled environmental conditions (temperature: 25 ± 2°C; 12-hour light/dark cycle) with *ad libitum* access to water and specialized chow. The experimental design was approved by the Institutional Ethics Committee on the Use of Animals at UFMG (Protocol N°. 389/2016).

Dietary model and pharmacological intervention: A formal *a priori* sample size calculation or power analysis was not performed. The experimental design was derived from the foundational model established by Castor⁹ which demonstrated that an isocaloric diet induces cardiac dysfunction via activation of the NLRP3 (NOD-like receptor family pyrin-domain-containing 3) inflammasome. The high-carbohydrate formulation comprised 45% ground commercial rodent chow, 45% Nestlé® condensed milk, and 10% União® refined sugar,²³ verified as isocaloric relative to a standard diet supplemented with 30% sucrose. To evaluate the functional role of the NLRP3 inflammasome, mice were treated with glibenclamide, a validated inhibitor of NLRP3 activation,²⁴ at dosages of 5 and 20 mg/kg. Following an initial four-week period of high-carbohydrate dietary preconditioning, the mice were allocated into either a control group (receiving vehicle: 0.9% saline solution containing 0.5% carboxymethylcellulose) or a treatment group (receiving 20 mg/kg glibenclamide).²⁵ The respective formulations were administered daily via oral gavage for an additional four weeks while maintaining the dietary regimens.

Tissue processing and protein extraction: Following the eight-week experimental period, mice were euthanized via decapitation under deep general anesthesia (80 mg/kg ketamine and 10 mg/kg xylazine). The whole cerebella were rapidly dissected and preserved at -30°C. For protein extraction, individual tissue samples were homogenized

on ice for 2 minutes using a mechanical mini-pestle in lysis buffer consisting of 25 mM Tris-HCl (pH 7.5), 10 mM EDTA, 2 mM DTT, and 0.5 mM PMSF, yielding a final suspension volume of 500 µL per sample. The crude homogenates were centrifuged at 4,500 rpm for 10 minutes at room temperature. The pellet was discarded and the protein-rich supernatant collected. A small aliquot was set aside for total protein quantification, while the remaining volume was diluted in distilled water and mixed with 20 µL of a 10X sample loading buffer (composed of 75% SDS, 20% sucrose, 31 mM equilibrium buffer, 19% β-mercaptoethanol, 11 mM EGTA-K, and 0.25% bromophenol blue). The samples were subsequently denatured by heating at 100°C for 2 minutes.

Biochemical and densitometric analysis: Total protein concentrations were determined via the Bradford spectrophotometric method (1976). A standard reference curve was prepared using bovine serum albumin (BSA, 0.1 mg/mL) across a linear range of 0, 5, 10, 15, and 20 µg. Duplicate 10 µL aliquots of the experimental samples were incubated with 3 mL of Bradford reagent, homogenized, and analyzed at an absorbance wavelength of 595 nm. Linear regression analysis was executed using Microsoft Excel® to calculate absolute protein concentration (µg/µL).

Proteins were resolved using one-dimensional sodium dodecyl sulfate-polyacrylamide gel electrophoresis (1D SDS-PAGE) under a discontinuous buffer system. The resolving gel consisted of a 12.5% acrylamide matrix prepared in 1.5 M Tris-HCl buffer (pH 8.8) with 10% SDS, acrylamide/bisacrylamide (30:0.8), TEMED, and 10% ammonium persulfate (APS). The stacking gel comprised a 3% acrylamide matrix in 0.5 M Tris-HCl buffer (pH 6.8) with 10% SDS, acrylamide/bisacrylamide (30:1.6), TEMED, and 10% APS.²⁶ Each lane was loaded with exactly 20 µg of total protein. Electrophoretic separation was driven by a constant current of 25 mA in a standard running buffer (250 mM Tris, 1.92 M glycine, 1% SDS). Resolved gels were stained overnight in Coomassie Brilliant Blue R solution (0.125% Coomassie Blue, 50% methanol, 10% acetic acid) and subsequently cleared in a destaining solution (25% ethanol, 10% methanol, 9% acetic acid) before long-term storage in 4% acetic acid.

The relative mobility (R_f) of individual protein bands was determined relative to a commercial molecular weight (MW) ladder. Gels were sealed between 3 mm transparent protective films and digitized in uncompressed BMP format. Densitometric quantification of band intensities was performed using Scion Image Software® (version Alpha 4.0.3.2) to yield the Optical Density Index (ODI) for each target band. Statistical significance was verified via a paired Student's t-test using BioEstat 5.0 software, with alpha set at $p < 0.05$. Descriptive statistics are presented as mean ± standard deviation.

In Silico protein identification and function annotation: Protein identities matching the resolved molecular mass bands were predicted using the comprehensive quantitative proteomic database published by Kim et al. (2020) as a primary reference, which allowed the assignment of two or more candidate proteins per band. Functional annotations and canonical metadata were retrieved from UniProtKB (<https://www.uniprot.org>), filtered specifically for reviewed records within the *Mus musculus* proteome. The candidate protein list was further cross-referenced with DrugBank (<https://go.drugbank.com/>) and the Reactome Pathway Knowledgebase (<https://reactome.org/>) to standardize nomenclature and map biochemical pathways. The use of artificial intelligence technologies was restricted to the revision of the English language in the abstract, respectively, through DeepL, as well as the organization of the study's bibliographies using NotebookLM.

Results and discussion

The electrophoretic profiles of the cerebellar supernatants revealed eight distinct, highly reproducible protein bands that were differentially expressed across the experimental cohorts: control mice receiving vehicle water (CV), mice receiving glibenclamide alone (CD), mice maintained exclusively on the refined carbohydrate-rich diet (DV), and mice subjected to the combined diet and glibenclamide regimen (DD). The apparent molecular masses of these bands were calculated via linear regression as 55.8, 51.4, 45.4, 41.8, 36.9, 35.4, 28.8, and 26.5 kDa, and were sequentially designated as P1 through P8 (Figure 1).

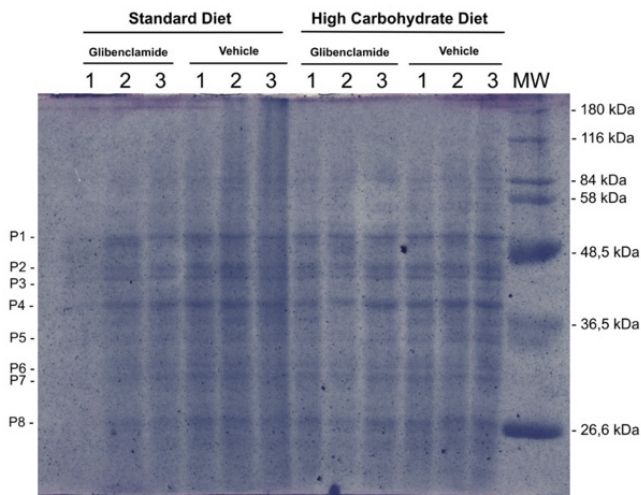


Figure 1 Electrophoretic profile of cerebellum samples from three mice from the groups treated only with glibenclamide (CD), only with water (CV), with a refined carbohydrate-rich diet and glibenclamide (DD), and only with a refined carbohydrate-rich diet (DV). P1 to P8 – Differentially expressed bands. MW – Molecular weight marker in kDa.

To evaluate changes in expression, the mean Optical Density Index (ODI) of each band was compared using a Student's t-test between the baseline CV group and the independent CD and DV groups, as well as between the CD cohort and the double-treated DD cohort. Statistically

significant alterations ($p < 0.05$) were confirmed for bands P1, P3, P6, P7, and P8. Specifically, glibenclamide alone significantly suppressed the baseline expression of P1 ($p=0.016$) and P3 ($p=0.026$), whereas the high-carbohydrate diet markedly increased their abundance. Band P6 expression was significantly downregulated by both glibenclamide (CD; $p=0.019$) and dietary stress (DV; $p=0.044$) independently. Interestingly, band P7 expression was reduced exclusively by glibenclamide administration ($p=0.043$), whereas band P8 ($p=0.039$) was up-regulated uniquely in response to the high-carbohydrate diet (Figure 2).

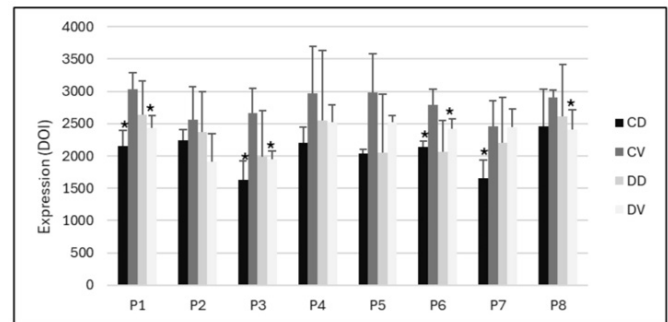


Figure 2 Mean optical densitometry index (ODI) and standard deviation (y-axis) for each differential protein (x-axis) present in cerebellum samples from mice in the groups treated only with glibenclamide (CD), only with water (CV), with a refined carbohydrate-rich diet and glibenclamide (DD), and only with a refined carbohydrate-rich diet (DV). P1 to P8 – Differentially expressed bands ($p < 0.05$).

Predictive bioinformatic modeling revealed that the cerebellar proteome exhibits remarkable functional diversity under these metabolic and pharmacological pressures. Categorization of the candidate proteins indicated that a large proportion are involved in nucleic acid processing, with 28.2% directly mapping to DNA and RNA metabolic events (Table 1). The remaining candidate proteins were distributed across general metabolic pathways (23.1%; Table 2), core cellular processes including apoptosis, proliferation, differentiation, and vesicular trafficking (15.4%), cell membrane dynamics (12.8%), protein folding and degradation (10.2%), lipid metabolism (7.7%), and carbohydrate metabolism (2.6%).

Table 1 Putative assignment of differentially expressed protein bands participating in DNA and RNA events based on *in silico* analysis using the UniProt accession code, name, function, and predicted molecular mass in kDa

Protein	Uniprot ID	Protein name	Protein function	MW
P1	Q99M31	Heat shock 70 kDa protein 14	Acts as a core component of the ribosome-associated complex (RAC); actively involved in folding nascent polypeptides and maintaining them in folding-competent conformations.	55.8
P3	O08580	Steroid hormone receptor ERR1	Orphan nuclear receptor that binds specifically to the ERR-alpha response element (5'-TNAAGGTCA-3') to modulate transcriptional activity.	45.4
P4	Q80UY2	E3 ubiquitin-protein ligase KCMF1	Accepts activated ubiquitin from E2 conjugating enzymes and transfers it to specific substrates, promoting their polyubiquitination and proteasomal degradation.	41.8
	Q91VA6	Polymerase delta-interacting protein 2	Regulates translesion DNA synthesis across template lesions, maintaining DNA integrity and damage tolerance.	
P5	Q99J09	Methylosome protein WDR77	Non-catalytic component of the methylosome complex; plays a foundational role in the regulation of gene transcription.	36.9
	Q920Q6	RNA-binding protein Musashi homolog 2	Post-transcriptionally regulates target mRNA translation; required for stem cell proliferation and maintenance in the central nervous system.	
	Q64705	Upstream stimulatory factor 2	Transcription factor that binds symmetrical E-box DNA sequences (5'-CACGTG-3') found within various viral and cellular promoters.	

Table I Continued...

P6	Q9D0Q7	Large ribosomal subunit protein mL45	Structural component of the mitochondrial large (39S) ribosomal subunit, assisting in mitochondrial translation.	35.4
	Q99N93	Large ribosomal subunit protein uL16m	Essential structural component of the mitochondrial ribosome; facilitates RNA binding and coordinates mitochondrial protein translation.	
P7	P17918	DNA sliding clamp PCNA	Encircles DNA to confer high processivity to DNA polymerases during leading-strand replication and coordinates DNA repair pathways.	28.8
	P70122	Ribosome maturation protein SBDS	Required for core ribosome biogenesis and the functional assembly of mature, translation-competent 60S ribosomal subunits.	

Table 2 *In silico* functional prediction of differentially expressed cerebellar protein bands involved in miscellaneous metabolic and cellular events

Protein	Uniprot ID	Protein name	Protein function	MW
P1	P24547	Inosine-5'-monophosphate dehydrogenase 2	Catalyzes the conversion of inosine 5'-phosphate to xanthosine 5'-phosphate, with important role in the regulation of cell growth.	55.8
P2	Q3UHG7	DENN domain-containing protein 11	Functions as a guanine nucleotide exchange factor (GEF) that converts inactive GDP-bound small GTPases into their active GTP-bound forms.	51.4
	Q8R1S0	Ubiquinone biosynthesis monooxygenase COQ6, mitochondrial	Mitochondrial enzyme required for two non-consecutive hydroxylation steps during the biosynthesis of ubiquinone (Coenzyme Q).	
P4	Q91WU5	Arsenite methyltransferase	Catalyzes the sequential transfer of methyl groups from S-adenosylmethionine to trivalent arsenicals, driving xenobiotic detoxification.	41.8
P5	Q9WVA3	Mitotic checkpoint protein BUB3	Essential component of the spindle assembly checkpoint; signals and promotes correct kinetochore-microtubule attachment.	36.9
P6	Q99L13	3-hydroxyisobutyrate dehydrogenase, mitochondrial	Mitochondrial enzyme that catalyzes the NAD ⁺ -dependent conversion of 3-hydroxy-2-methylpropanoate to 2-methyl-3-oxopropanoate during valine catabolism.	35.4
	Q91V61	Sideroflexin-3	Mitochondrial amino acid transporter that mediates the import of serine into the mitochondrial matrix for the one-carbon metabolism pathway.	
P8	Q9WTP6	Adenylate kinase 2, mitochondrial	Mitochondrial enzyme that catalyzes the reversible transfer of phosphate groups between ATP and AMP, maintaining adenine nucleotide homeostasis.	26.5
	Q8BHC4	Dephospho-CoA kinase domain-containing protein	Catalyzes the final ATP-dependent phosphorylation step in the canonical biosynthesis of Coenzyme A (CoA).	

Given the substantial functional diversity of the predicted candidates, a simple, monotonic correlation cannot link specific expression changes directly to a single pathophysiological pathway. Nonetheless, these data demonstrate that single-agent glibenclamide administration causes a profound down-regulation of bands P1 (55.8 kDa), P3 (45.4 kDa), P6 (35.4 kDa), and P7 (28.8 kDa) in mouse cerebellar tissue. This shifts from patterns reported in whole-brain proteomic models. For example, Faria¹² and Santos et al.²⁴ observed that a combined high-carbohydrate diet and glibenclamide intervention up-regulated three distinct protein bands with molecular masses of 44.8, 42.2, and 39.8 kDa, which were mapped respectively to phosphoglycerate kinase, the guanine nucleotide-binding protein Gs alpha-subunit, and fructose-bisphosphate aldolase.

Glibenclamide exerts its neuroprotective actions within the cerebellum primarily by blocking ATP-sensitive potassium (K_{ATP}) channels embedded in the plasma membrane, thereby adjusting neural excitability and attenuating acute ischemic or metabolic injury.²⁷ Clinical imaging data compiled by Fendler et al.¹¹ demonstrated that glibenclamide treatment improves cerebellar perfusion, a phenomenon mediated by the closure of neuronal K_{ATP} channels, which drives localized electrical activity and subsequent neurovascular coupling to increase regional blood flow. In developmental models, sulfonylurea receptors display very low density in the cerebellum at birth but mature rapidly during the first two postnatal weeks to match adult baseline levels.¹³ In isolated, cannulated cerebellar artery models, glibenclamide administration suppresses fixed vasodilatory responses

by approximately 50%.²⁸ Furthermore, glibenclamide selectively restricts hyperperfusion triggered by acute hypoxia across all major brain structures, including the cerebellum, while leaving baseline perfusion under normoxic or hemodiluted conditions unaffected, confirming that K_{ATP} channels help limit excessive, potentially damaging shifts in blood flow during hypoxic stress.²⁹

Experimental findings regarding glibenclamide's neuroprotective threshold in the cerebellum remain nuanced. Zheng and Zuo³⁰ reported that glibenclamide does not directly alter the survival of cerebellar Purkinje cells preconditioned with isoflurane or subjected to oxygen-glucose deprivation (OGD). Conversely, Yuan et al.³¹ demonstrated that administering glibenclamide during hypothermic preconditioning fully abolishes the expected reduction in Purkinje cell death following OGD. This block indicates that ischemic tolerance driven by hypothermia relies on active K_{ATP} channel configuration.

The down-regulation of protein bands P1, P3, P6, and P7 following isolated glibenclamide exposure suggests a coordinated shift in cerebellar homeostatic maintenance. Because our bioinformatic prediction primarily links these specific molecular mass ranges to ribosomal structural components and transcriptional adapters, it is highly probable that K_{ATP} channel blockade suppresses regional baseline protein synthesis. This targeted reduction in translation machinery may represent a metabolic conservation mechanism, minimizing non-essential energy expenditure in highly specialized cells like Purkinje neurons. The absence of a parallel downregulation in the combined DD cohort suggests that a high-carbohydrate background creates

a metabolic counter-pressure, effectively preserving translational infrastructure at the expense of metabolic equilibrium.

Furthermore, Fendler et al.¹¹ described that in patients carrying activating mutations in the *KCNJ11* gene (which encodes Kir6.2 of the K_{ATP} channels), glibenclamide promotes improvement in cerebellar blood flow, attenuating neurological symptoms such as intellectual disability, motor alterations, and epilepsy associated with permanent neonatal diabetes.

In parallel, the refined carbohydrate-rich diet introduced marked expression changes, up-regulating bands P1, P3, and P8, while selectively down-regulating P6. Interestingly, separate whole-brain proteomic analyses using identical dietary protocols failed to detect significant shifts in total protein expression when comparing control groups directly against carbohydrate-challenged groups.^{21,22} This discrepancy indicates that the cerebellum possesses a unique molecular vulnerability (or a highly specialized compensatory mechanism) relative to other brain regions.

Thus, the diet rich in refined carbohydrates demonstrated heterogeneous effects, increasing the expression of P1, P3, and P8, but reducing P6. In studies with mouse brain, Santos²² and Santos et al.²¹ did not detect significant alterations in differential protein expression when comparing groups with and without dietary intervention.

Different dietary patterns may distinctly impact the nervous system, encompassing both brain and cerebellar structures. Obesogenic diets, for example, promote selective carbonylation of proteins involved in ATP homeostasis and glutamate metabolism in the cerebellum, while supplementation with fish oil limits the carbonylation of proteins oxidatively damaged by the obesogenic diet, providing protection against the carbonylation of several proteins involved in biosynthesis and amino acid neurotransmission.¹⁶ On the other hand, experiments with pregnant female pigs fed a diet enriched with docosahexaenoic acid resulted in offspring with elevated concentrations of this polyunsaturated fatty acid in the prefrontal cortex and cerebellum.³² Additionally, an experiment with a ketogenic diet showed a global reduction in cerebral glucose metabolism, with regional variations.¹⁷

Diets rich in sugars do not modify acetylcholinesterase activity in the cerebellum, indicating no interference in the degradation of acetylcholine in this region, although they affect other structures such as the hippocampus, cortex, and hypothalamus.¹⁹ Lastly, severe nutritional restrictions, such as an isocaloric low-protein diet (8%) during gestation and lactation, significantly deplete absolute cerebellar DNA concentration in offspring, confirming that macronutrient imbalances can disrupt normal neuronal development and structural assembly.^{15,33,34}

Final considerations

This study investigated the cerebellar protein profiles of Balb/c mice subjected to an eight-week refined carbohydrate-rich diet and evaluated the modulatory effects of glibenclamide pharmacotherapy. Eight differentially expressed protein bands were identified across all cohorts. Five of these bands demonstrated statistically significant alterations. *In silico* analysis mapped these responsive bands primarily to core DNA and RNA processing pathways, alongside secondary networks governing apoptosis, proliferation, cellular differentiation, intracellular signaling, and vesicular trafficking.

Individually, single-agent glibenclamide administration significantly reduced the expression of three protein bands, whereas the isolated high-carbohydrate diet up-regulated three bands. Only

one band displayed a concurrent decrease when both treatments were combined. These findings reveal that while a combined regimen does not cause additive or synergistic shifts in protein expression, both interventions independently alter the cerebellar proteome. This distinct separation raises important questions regarding how therapeutic agents and metabolic pressures interact at the molecular level within central nervous tissues.

Given that refined carbohydrate diets drive systemic metabolic diseases like type 2 *diabetes mellitus* (which is routinely treated with glibenclamide) mapping these proteomic adjustments is essential. It supports more integrated therapeutic approaches for complex, multifactorial diseases such as diabetes, obesity, systemic hypertension, rheumatoid arthritis, and Alzheimer's disease.

We acknowledge several methodological limitations in this study:

- I. Pipetting variance during initial tissue processing may have introduced minor errors in total protein quantification;
- II. While one-dimensional SDS-PAGE provided an accessible, cost-effective method for protein separation, it inherently collapses multiple proteins of similar molecular mass into single bands. Transitioning to high-resolution two-dimensional electrophoresis would resolve these co-migrating species, though it demands higher financial and operational support;
- III. Technical limits in polyacrylamide gel resolution occasionally obscured faint bands, restricting precise optical density measurements;
- IV. The modest sample size may have constrained overall statistical power, highlighting the need for larger-scale replication studies;
- V. The scarcity of specialized cerebellar proteomic literature necessitated reliance on a single primary reference database for candidate identification, creating multiple matching possibilities and precluding definitive functional correlations;
- VI. Scarce literature regarding carbohydrate-induced cerebellar remodeling limited the depth of comparative discussions.

Consequently, further targeted research into cerebellar proteomics under nutritional and pharmacological stress is needed. Downstream metabolomic profiling could provide an integrated view of these macromolecular shifts, while high-throughput liquid chromatography-tandem mass spectrometry (LC-MS/MS) would allow definitive protein identification and deep characterization across all experimental groups. The distinct protein bands identified here represent promising candidates for advanced proteomic characterization and structural *in silico* modeling.

Acknowledgments

This study was supported in part by the Coordenação de Aperfeiçoamento de Pessoal de Nível Superior (CAPES), and by the Fundação de Amparo à Pesquisa do Estado de Minas Gerais (FAPEMIG, Project No. APQ-02768-17), which provided the research scholarship to RGMC. The authors thank the Federal University of Minas Gerais (UFMG) and the Federal University of Uberlândia (UFU) for institutional support, and for the scholarship granted to ILS (DIREN/PET 050/2025) via the Tutorial Education Program (PET Bio Pontal). The authors also express their gratitude to Dr. Foued Salmen Espindola (Federal University of Uberlândia) for providing the one-dimensional electrophoresis equipment and donating essential chemical reagents.

Conflicts of interest

The authors declare that no conflicts of interest exist regarding the publication of this study.

References

1. Brasil. Ministério da Saúde. Secretaria de Vigilância em Saúde e Ambiente. Cenário da obesidade no Brasil. Boletim Epidemiológico, Brasília, DF. 2024;55(7).
2. Brasil. Ministério da Saúde. Secretaria de Vigilância em Saúde e Ambiente. Vigitel Brasil 2006-2024: vigilância de fatores de risco e proteção para doenças crônicas por inquérito telefônico. Brasília: Ministério da Saúde, 2025. 211 p.
3. Polacow Viviane Ozores, Lancha Junior Antonio Herbert. Dietas hiperglicídicas: efeitos da substituição isoenergética de gordura por carboidratos sobre o metabolismo de lipídios, adiposidade corporal e sua associação com atividade física e com o risco de doença cardiovascular. *Arquivos Brasileiros de Endocrinologia & Metabologia, São Paulo*. 2007;51(3):389–400.
4. Ludwig David S, Friedman Mark I. Increasing Adiposity: Consequence or Cause of Overeating?. *JAMA Chicago*. 2014;311(210):2167.
5. Bikman Benjamin T, Kim J. Shimy, Caroline M. Apovian, et al. A high-carbohydrate diet lowers the rate of adipose tissue mitochondrial respiration. *European Journal of Clinical Nutrition, London*. 2022;76:1339–1342.
6. Franco Claudinéia Conationi da Silva, Kelly V Prates, Carina Previante, et al. Glibenclamide treatment blocks metabolic dysfunctions and improves vagal activity in monosodium glutamate-obese male rats. *Endocrine, New York*. 2017;56(2):346–356.
7. Tsarenko Sergey Vladimirovich, Dzyadz'ko Alexander Mikhailovich, Rybalko Sergey Sergeevich. Glibenclamide as a promising agent for prevention and treatment of cerebral edema. *Zhurnal voprosy neurokhirurgii imeni NN Burdenko*. 2017;81(3):88–93.
8. Zubov Alexander, Zamira Muruzheva, Maria Tikhomirova, et al. Glibenclamide as a neuroprotective antidementia drug. *Archives of Physiology and Biochemistry*. 2022;128(6):1693–1696.
9. Castor Renata Gomes Miranda E. *Efeitos Da Glibenclamida Sobre A Ativação Cardíaca De Inflamassoma NLRP3 Induzida Por Dieta Rica Em Carboidratos Refinados*. Dissertação (Mestrado Em Fisiologia E Farmacologia) - Universidade Federal De Minas Gerais, Belo Horizonte, 2019. p. 64.
10. Tai Kwok-Keung, Pham Ly, Truong Daniel D. Intracisternal administration of glibenclamide or 5-hydroxydecanoate does not reverse the neuroprotective effect of ketogenic diet against ischemic brain injury-induced neurodegeneration. *Brain Injury*. 2009;23(13-14):1081–1088.
11. Fendler, Wojciech, Iwona Pietrzak, Melissa F Brereton, et al. Switching to sulphonylureas in children with iDEND syndrome caused by KCNJ11 mutations results in improved cerebellar perfusion. *Diabetes Care, Alexandria*. 2013;36(8):2311–2316.
12. Faria Sttefany Nayara Sant'ana de. *Proteínas diferencialmente expressas no cérebro após dieta rica em carboidratos refinados e tratamento com glibenclamida*. Trabalho de Conclusão de Curso (Graduação em Ciências Biológicas) – Universidade Federal de Uberlândia, Ituiutaba, 2023. p. 27.
13. Xia Ying, Eisenman David, Haddad Gabriel G. Sulfonylurea receptor expression in rat brain: effect of chronic hypoxia during development. *Pediatric Research*. 1993;34:634–641.
14. Kandel Eric Richard. *Princípios de Neurociências*. Tradução: Ana Lúcia Severo et al. 5th edn. Porto Alegre: AMGH Ltda, 2014. p. 833–851.
15. Bennis-Taleb Nadia, Claude Remacle, Joseph J Hoet, et al. A low-protein isocaloric diet during gestation affects brain development and alters permanently cerebral cortex blood vessels in rat offspring. *The Journal of Nutrition, Bethesda*. 1999;129(8):1613–1619.
16. Moreno Francisco, Lucía Méndez, Ana Raner, et al. Dietary marine oils selectively decrease obesogenic diet-derived carbonylation in proteins involved in ATP homeostasis and glutamate metabolism in the rat cerebellum. *Antioxidants (Basel), Basileia*. 2024;13(1):103.
17. Horowitz Tatiana, Emilie Doche, Mary Philip, et al. Regional brain glucose metabolism is differentially affected by ketogenic diet: a human semi-quantitative positron emission tomography. *European Journal of Nuclear Medicine and Molecular Imaging, Berlin*. 2023;50:2047–2055.
18. Ziegler Denize R, Araújo Emeli, Rotta Liane N, et al. A ketogenic diet increases protein phosphorylation in brain slices of rats. *The Journal of Nutrition*. 2002;132(3):483–487.
19. Kaizer Rosilene Rodrigues, Adriane C da Silva, Vera M Morsch, et al. Diet-induced changes in Ache activity after long-term exposure. *Neurochemical Research, New York*. 2004;29(12):2251–2255.
20. Kim Yong Gyu, Jongmin Woo, Joonho Park, et al. Quantitative proteomics reveals distinct molecular signatures of different cerebellum-dependent learning paradigms. *Journal of Proteome Research, Washington*. 2020;19(5):2011–2025.
21. Santos Paula Viana Sene dos, Sttefany Nayara Sant'Ana de Faria, Renata Gomes Miranda e Castor, et al. Glibenclamide alters the brain protein profile and morphometry of hippocampal regions in mice fed with a high-refined carbohydrate diet. *Open Access Journal of Science*. 2024;7(1):160–167.
22. Santos Paula Viana Sene dos. *Análise eletroforética de proteínas do cérebro de camundongos tratados com dieta rica em carboidratos refinados*. Trabalho de Conclusão de Curso (Graduação em Ciências Biológicas) – Universidade Federal de Uberlândia, Ituiutaba, 2023. p. 29.
23. Marina C Oliveira, Zélia Menezes-Garcia, Milene CC Henriques, et al. Acute and sustained inflammation and metabolic dysfunction induced by high refined carbohydrate-containing diet in mice. *Obesity, Silver Spring*. 2013;21(9):396–406.
24. Lamkanfi Mohamed, James L Mueller, Alberto C Vitari, et al. Glyburide inhibits the cryopyrin/Nalp3 inflammasome. *The Journal of Cell Biology, New York*. 2009;187(1):61–70.
25. Jian Cai, Shuai Lu, Zheng Yao, et al. Glibenclamide attenuates myocardial injury by lipopolysaccharides in streptozotocin-induced diabetic mice. *Cardiovascular Diabetology, London*. 2014;13(1).
26. Laemmli Ulrich K, Teaff Norman, D'ambrosia J. Maturation of the head of bacteriophage T4. III. DNA packaging into preformed heads. *Journal of Molecular Biology, London*. 1974;88(4):749–765.
27. Zhou Fangfang, Yangjun Liu, Binbin Yang, et al. Neuroprotective potential of glibenclamide is mediated by antioxidant and anti-apoptotic pathways in intracerebral hemorrhage. *Brain Research Bulletin*. 2018;142:18–24.
28. Koide Masayo, Arsalan U Syed, Karen M Braas, et al. Pituitary adenylate cyclase activating polypeptide (PACAP) dilates cerebellar arteries through activation of large-conductance Ca(2+)-activated (BK) and ATP-sensitive (K ATP) K (+) channels. *Journal of Molecular Neuroscience, Totowa*. 2014;54(3):443–450.
29. Tomiyama Yoshinobu, Brian JR Johnny E, Todd Michael M. Cerebral blood flow during hemodilution and hypoxia in rats: role of ATP-sensitive potassium channels. *Stroke*. 1999;30(9):1942–1948.
30. Zheng Shuqiu, Zuo Zhiyi. Isoflurane preconditioning reduces purkinje cell death in an in vitro model of rat cerebellar ischemia. *Neuroscience*. 2023;118(1):99–106.

31. Yuan Hui-Bih, Huang Yueming, Zheng Shuqiu, et al. Hypothermic preconditioning increases survival of Purkinje neurons in rat cerebellar slices after an in vitro simulated ischemia. *Anesthesiology*. 2004;100(2):331–337.
32. Stephanie Dubrof, Jillien G Zukaitis, Ishfaque Ahmed, et al. The effect of perinatal supplementation of DHA on specialized pro-resolving lipid mediators in the brain of offspring. *Biochimica et Biophysica Acta (BBA) - Molecular and Cell Biology of Lipids, Amsterdam*. 2025;1870(5):159629.
33. Bradford Marion Mckinley. A rapid and sensitive method for the quantitation of microgram quantities of protein utilizing the principle of protein-dye binding. *Analytical Biochemistry, New York*. 1976;72(1-2):248–254.
34. Renata Gomes Miranda e Castor, Alexandre Santos Bruno, Camila André Pereira, et al. Glibenclamide reverses cardiac damage and NLRP3 inflammasome activation associated with a high refined sugar diet. *European Journal of Pharmacology, Amsterdam*. 2024;984:177035.